Virtual Histology of the Heart Through CT Imaging: Preliminary Results of a Novel Noninvasive Approach for Cardiac Tissue Characterization

Riccardo Forni[1,2], Carmine Gelormini[1], Cristiana Corsi[2], Paolo Gargiulo[1,3]

[1] Institute of Biomedical and Neural Engineering, Reykjavik University, Reykjavik, Iceland
[2] Department of Electrical, Electronic and Information Engineering, University of Bologna, Cesena, Italy
[3] Department of Science, Landspitali, University Hospital of Iceland, Reykjavik, Iceland

Abstract

The world's population is aging and cardiovascular diseases can become the first cause of frailty in the next future. This study proposes a novel workflow to measure cardiac tissue quality and composition from a CT scan directly through the Hounsfield Units distribution of 3D samples. The cohort includes 15 healthy subjects to study normal heart densitometric composition and 7 hypertrophic patients to measure how the pathology affects myocardial tissue. A significative fat content of 3% of the volume is found in the hypertrophic free wall while the connective tissue in the septum changed from just above 1% to around 5%. Therefore, the proposed noninvasive approach might become a clinical marker to improve diagnosis derived from CT imaging.

1. Introduction

Strategies to tackle cardiovascular diseases (CVD) become crucial as the population ages. Nowadays, people present multiple comorbidities, and CVDs could lead to a condition of frailty with a compromised quality of life [1]. On the other hand, the number of children and adolescents with hypertension is not decreasing making them prone to develop CVDs, and particularly hypertrophic cardiomyopathy (HCM) [2]. In a scenario of evolution and with disease stratifications, having more markers to track pathology development is necessary.

Imaging techniques (echocardiography, cardiac magnetic resonance imaging and cardiac computed tomography) can investigate both morphological and functional aspects such as wall size and motion, presence of scars, narrowing of coronaries, presence of calcifications and others. Direct information about tissue content and quality are still lacking. In particular, computed tomography is already used to extract measurements about soft tissue from the Hounsfield unit (HU) distributions.

Edmunds et al. compared the HU distributions from a cross-section of the midthigh to investigate tissue composition among young individuals, elders and subjects with sarcopenia [3]. The trimodal profile was then used on a large dataset to compute the quantity of fat, connective and muscular tissue and relate them with self-reported and instrumentally measured biometric features [4,5]. In a longitudinal study using the same parameters from the midthigh authors were able to predict CVD, chronic heart failure and coronary heart disease [6].

The objective of the study is to understand if a novel approach of virtual histology based on HU distribution applied to cardiac tissue of the left ventricle can describe cardiac muscle status and detect the presence of pathologies modifying myocardial tissue.

2. Materials & Methods

2.1. Population

The cardiac volume database comprised 22 subjects: 15 healthy and 7 with obstructive HCM. 15 static CT data were acquired with a Revolution Evo GE Healthcare machine with a $100kV$ radiogenic tube. 7 static CT data were acquired with a Canon Medical System Aquilion ONE machine with a $120kV$ radiogenic tube. Pixel size (PS) was in $0.4 - 0.5mm$ range and slice thickness (ST) between 0.25 and $0.6mm$ with a field of view (FOV) of $200 - 250mm$.

2.2. Cardiac CTs segmentation and parameters extraction

We propose a novel workflow (Figure 1) to extract 3D samples from the external wall of the left ventricle (LVFW) and the interventricular septum (IVS) and to analyze tissue composition based on the HU distributions.
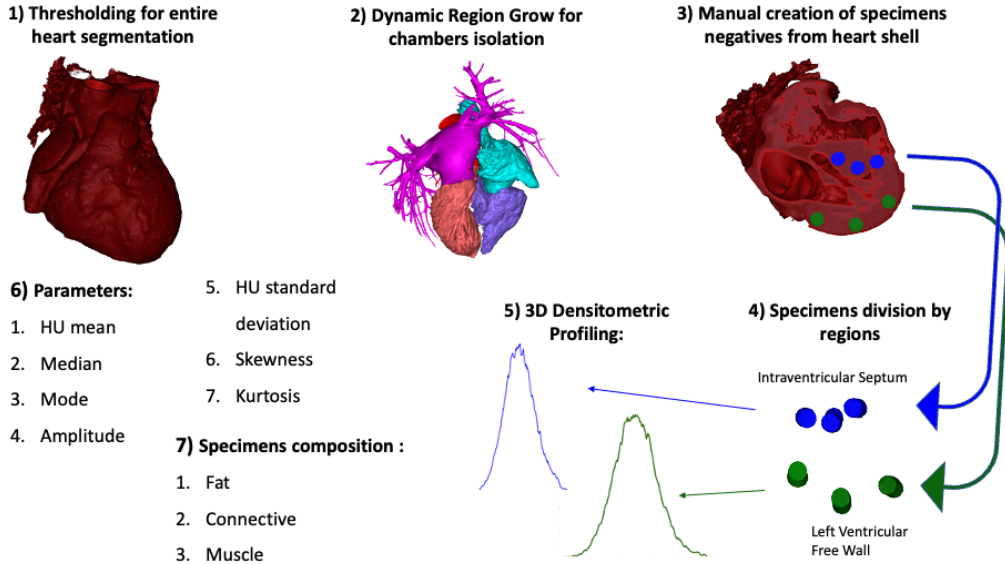Image analysis was performed in Mimics 23.0 software

Figure 1: Novel workflow for densitometric parameters extraction and tissue composition analysis.

(Materialise, Leuven, Belgium). A mask for the entire myocardium in $[-200; 1600]$ HU range was created (Fig 1, panel 1).

Simultaneously, a mask for each heart chamber was obtained based on different pixel intensities and dynamic region-grown algorithms. (Fig 1, panel 2) A boolean subtraction of heart chamber masks from the first one was performed to isolate the myocardium shell from the blood pool. The selection of the 3D cylindrical samples (volumes of interest, VOIs) was designed. Six 3D holes were manually drawn from a copy of the heart shell mask; then by applying a boolean subtraction from the original mask the specimens were generated (Fig 1, panel 3). The VOIs were drawn above and below the four-chamber view in the axial plane: three were selected on the IVS, and the other 3 on the LVFW. In each region, one specimen was taken close to the valvular plane, one at the apex and one at the midpoint between them (Fig 1, panel 4).

The volume of each specimen was computed as:

$$SampleVolume = \frac{\pi}{4} * D^2 * PS^2 * ST * NSlices \quad (1)$$

where D is the diameter of the cylinder section and $NSlices$ is the number of slices and the six VOIs were selected for further analysis if their volume was $1[cc]$ with a tolerance of 15%. If this constraint was not fulfilled, the specimen selection was repeated. The HU values were then exported.

For each subject, a densitometric profile, a histogram of the HU distribution normalized to the total number of pixels, was drawn for both regions (Fig 1, panel 5). From the Gaussian-shaped profile, seven parameters were computed and used to create a densiometric profile: HU mean, median and mode measure the average CT absorption value of cardiac specimens; peak amplitude and HU standard deviation (HU std) assess the arrangement of muscle, fat and connective tissue components, as well as skewness and kurtosis (Fig 1, panel 6). In a second study concerning tissue composition, the percentages of fat ($[-200; -20]$ HU), connective tissue ($[-20; +20]$ HU) and muscle ($> +20$ HU) were extracted from the densitometric profile (Fig 1, panel 7). Thresholds are based on previous studies and experimental data [7, 8].

2.3.   Statistical analysis

Data were analyzed using a linear mixed model, a generalization of the linear regression model, relaxing the assumption that the errors are independent and therefore, uncorrelated. Since our experimental design had multiple measurements from different regions within each subject, correlation within-subject data had to be accounted for [9]. R [10] and lme4 [11] were used to perform a linear mixed model with the seven densitometric parameters as dependent variables and pathology and region as fixed effects. Interaction effects between independent variables were also considered. We specified a model with a random intercept and unstructured covariance structure using Restricted Maximum Likelihood (REML). $P - values < 0.05$ were considered statistically significant and Satterthwaite's approximation was implemented to calculate degrees of freedom [12].

The assumption of normality was checked using the Shapiro-Wilk test of normality. Additionally, to further explore any significant effects identified in the previous analyses, we conducted simple contrast analyses with Bonferroni correction using the emmeans package.

3. Results

Intraventricular septum resulted a denser structure than the left ventricular free wall in the control group ($+15HU$, $p < 0.01$ with HU mean, mode and median), but not in the pathological subjects ($p > 0.05$), as shown in Figure 2. Shape parameters did not show any statistical difference among groups.
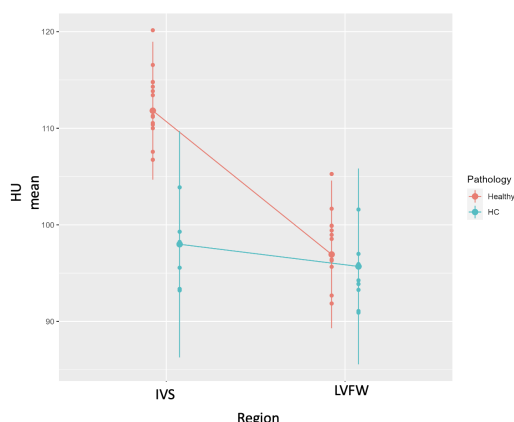

Figure 2: Densitometric parameter: HU mean as the output of the linear mixed model showing the higher density measured on IVS for the control (healthy) group. HCM showed a different densitometric behavior, having similar values on both IVS and LVFW.
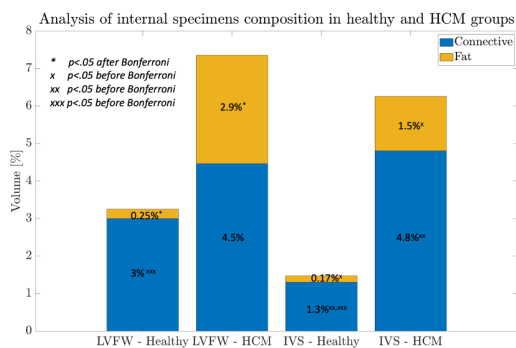

Figure 3: Tissue composition comparison: fat content is significantly higher in LVFW of HCM group whereas is absent in control group. Similar situation on IVS with lower percentages. Also the connective tissue increments with the pathology.

Fat and connective tissue percentages are reported in Figure 3. The control group reported less than 0.3% of fat in both regions. Connective tissue is around $3\% \pm 0.6\%$ in LVFW and drops to $1.3\% \pm 0.7\%$ on IVS. HCM group, instead, had less muscle with $2.90\% \pm 0.5\%$ fat and $4.5\% \pm 0.5\%$ connective in LVFW and $1.5\% \pm 0.7\%$ fat and $4.8\% \pm 0.5\%$ connective in IVS. The increase of fat in the LVFW in HCM group was statistically significant ($p < 0.001$), whereas the other comparisons lost the significance after Bonferroni correction (Figure 3, $*$ and ^{x} symbols).

Tissue composition changes could be seen from the 3D densitometric profile as shown in Figure 4.

4. Discussion

Our results obtained analyzing densitometric profiles showed IVS as a denser (HU mean, mode and median) tissue compared to LVFW, as confirmed by the anatomical references [13]. The different transmural fiber alignments did not seem to impact the measured parameters.

In HCM subjects differences between IVS and LVFW were not reported suggesting a characteristic densitometric value for both regions different from what was found in the control group. Indeed, due to different CT scanners, the lower density of IVS in the HCM group may not be due to the pathology.

Looking at the sample composition, there are no universally accepted threshold intervals. Among what is reported in the literature, authors agreed on: (1) a more conservative threshold for muscle ($+20$ HU); (2) a symmetrical range for connective tissue composed mainly of water around 0 HU and decided (3) to label everything below -20 HU as fat to have a realistic representation of what a normal septum is and what HCM hearts report. A statistical significance in the volume of fat is found among healthy and HCM, meaning that the signs (fibrosis with fat deposition [14]) may be assessed and quantified with the technique.

5. Conclusion

As far as we know, this is the first study proposing the use of virtual histology from CT imaging to evaluate densitometric parameters and assess cardiac tissue composition in healthy and diseased hearts. The comparison of fat and connective compounds between healthy and HCM subjects showed significant differences and might be considered be a marker to detect the presence of CVD. Following a more comprehensive validation on a larger population, also considering other cardiac diseases, the proposed non invasive approach might improve clinical diagnosis derived from CT imaging.
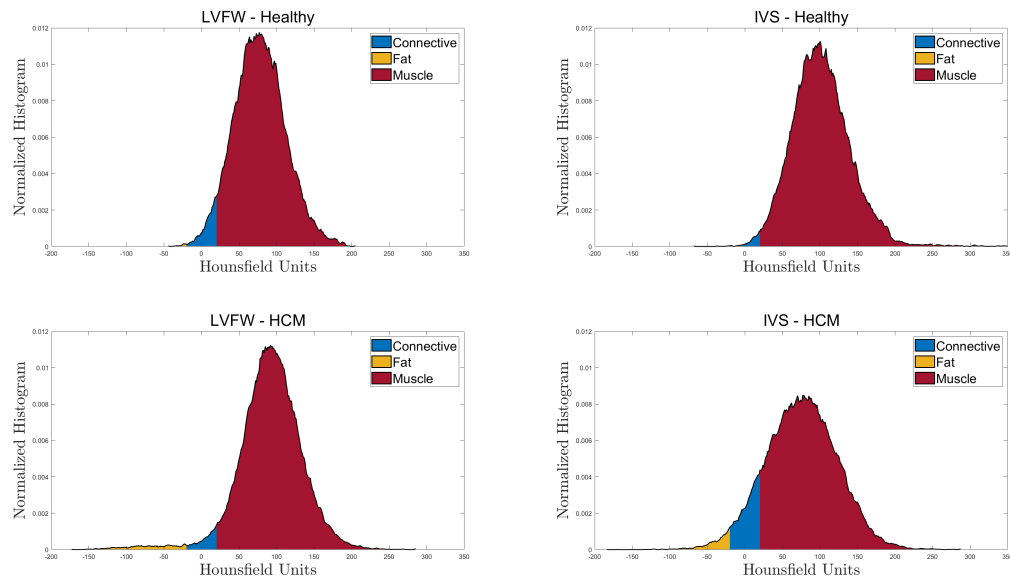
Figure 4: Patient-specific 3D profiles of a healthy subject (first row) and an HCM subject (second row). The three tissue types are drawn with different colors. A tail in the LVFW - HCM profile represents the presence of the pathology, the onset of non-muscular tissue. Also in IVS (right column), the pathological profile reports more fat tissue than the healthy one.

References

[1] Aïdoud A, Gana W, Poitau F, Debacq C, Leroy V, Nkodo JA, Poupin P, Angoulvant D, Fougère B. High prevalence of geriatric conditions among older adults with cardiovascular disease. Journal of the American Heart Association 2023; e026850.

[2] Kharbanda EO. Epidemiology of hypertension and cardiovascular disease in children and adolescents. Pediatric Hypertension 2023;367.

[3] Edmunds KJ, Árnadóttir Í, Gíslason MK, Carraro U, Gargiulo P. Nonlinear trimodal regression analysis of radiodensitometric distributions to quantify sarcopenic and sequelae muscle degeneration. Computational and Mathematical Methods in Medicine 2016;2016.

[4] Edmunds K, Gíslason M, Sigurdsson S, Gudnason V, Harris T, Carraro U, Gargiulo P. Advanced quantitative methods in correlating sarcopenic muscle degeneration with lower extremity function biometrics and comorbidities. PloS One 2018;13(3):e0193241.

[5] Recenti M, Ricciardi C, Edmunds KJ, Gislason MK, Sigurdsson S, Carraro U, Gargiulo P. Healthy aging within an image: Using muscle radiodensitometry and lifestyle factors to predict diabetes and hypertension. IEEE Journal of Biomedical and Health Informatics 2020;25(6):2103–2112.

[6] Ricciardi C, Edmunds KJ, Recenti M, Sigurdsson S, Gudnason V, Carraro U, Gargiulo P. Assessing cardiovascular risks from a mid-thigh ct image: a tree-based machine learning approach using radiodensitometric distributions. Scientific Reports 2020;10(1):1–13.

[7] Marwan M, Achenbach S. Quantification of epicardial fat by computed tomography: why, when and how? Journal of Cardiovascular Computed Tomography 2013;7(1):3–10.

[8] Mazonakis M, Damilakis J. Computed tomography: What and how does it measure? European Journal of Radiology 2016;85(8):1499–1504.

[9] Zuur AF, Ieno EN, Walker NJ, Saveliev AA, Smith GM, et al. Mixed effects models and extensions in ecology with R, volume 574. Springer, 2009.

[10] R Core Team R, et al. R: A language and environment for statistical computing 2013;.

[11] Bates D, Mächler M, Bolker B, Walker S. Fitting linear mixed-effects models using lme4. arXiv preprint arXiv14065823 2014;.

[12] Kuznetsova A, Brockhoff PB, Christensen RH. lmertest package: tests in linear mixed effects models. Journal of Statistical Software 2017;82:1–26.

[13] Triposkiadis F, Xanthopoulos A, Boudoulas KD, Giamouzis G, Boudoulas H, Skoularigis J. The interventricular septum: Structure, function, dysfunction, and diseases. Journal of Clinical Medicine 2022;11(11):3227.

[14] Maron BJ, Maron MS. Hypertrophic cardiomyopathy. The Lancet 2013;381(9862):242–255.

Address for correspondence:

Riccardo Forni
riccardo21@ru.is
Menntavegur 1, Reykjavik, 102, Iceland